Available online at www.sciencedirect.com

SCIENCE DIRECT

Biochimica et Biophysica Acta 1664 (2004) 53–63

BIOCHIMICA ET BIOPHYSICA ACTA
BBA

www.bba-direct.com

Association of sugar-based carboranes with cationic liposomes: an electron spin resonance and light scattering study

Sara Morandi[a], Sandra Ristori[a], Debora Berti[a], Luigi Panza[b], Aldo Becciolini[c], Giacomo Martini[a,*]

[a] *Dipartimento di Chimica, Laboratorio di Chimica Fisica delle Interfasi, Università di Firenze, 50019, Sesto Fiorentino no, Florence, Italy*
[b] *Dipartimento di Scienze Chimiche, Alimentari, Farmaceutiche, Farmacologiche, Università degli Studi del Piemonte Orientale, 28100 Novara, Italy*
[c] *Dipartimento di Fisiopatologia Clinica, Laboratorio di Biologia Cellulare e Radiobiologia, Università di Firenze, 50134 Florence, Italy*

Received 28 October 2003; received in revised form 7 April 2004; accepted 8 April 2004
Available online 10 May 2004

Abstract

The possibility of cationic (di-oleoyltrimethylammonium propane, DOTAP)/(L-α-dioleoylphosphatidyl-ethanolamine, DOPE) liposomes to act as carriers of boronated compounds such as 1,2-dicarba-*closo*-dodecaboran(12)-1-ylmethyl](β-D-galactopyranosyl)-(1 → 4)-β-D-glucopyranoside and 1,2-di-(β-D-gluco-pyranosyl-ox)methyl-1,2-dicarba-*closo*-dodeca-borane(12) has been investigated by Electron Spin Resonance (ESR) of *n*-doxyl stearic acids (*n*-DSA) and Quasi-Elastic Light Scattering (QELS). Both these carboranes have potential use in Boron Neutron Capture Therapy (BNCT), which is a targeted therapy for the treatment of radiation resistant tumors. They were shown to give aggregation both in plain water and in saline solution. Carborane aggregates were, however, disrupted when DOTAP/DOPE liposome solutions were used as dispersing agents. The computer analysis of the ESR spectra from carborane-loaded liposomes allowed to establish an increase of the order degree in the liposome bilayer with increasing carborane concentration, together with a decreased mobility. The same discontinuities of both correlation time and order parameter with respect to temperature variations were observed in carborane-containing and carborane-free liposomes. This suggested that a homogeneous dispersion of nitroxides and carboranes occurred in the liposome bilayer. The ESR line shape analysis proved that no dramatic changes were induced in the liposome environment by carborane insertion. QELS data showed that the overall liposome structure was preserved, with a slight decrease in the mean hydrodynamic radius and increase in polydispersity caused by the guest molecules.

Keywords: Carborane; Liposome; Electron spin resonance

1. Introduction

Boronated compounds are currently of great interest for their use in Boron Neutron Capture Therapy (BNCT) [1,2]. This is a targeted cancer therapy based on two separate steps: (i) accumulation of ^{10}B atoms into neoplastic tissues; (ii) irradiation with a thermal (or epithermal) neutron beam. Neutrons are able to induce fission of the ^{10}B nuclei, with consequent release of heavy particles:

$$^{10}B + n \rightarrow [^{11}B] \rightarrow {}^{7}Li + {}^{4}He + \gamma \quad (1)$$

The resulting lethal effect is limited to the cells where boron nuclei are located or to those in the nearest proximity, because the penetration length in tissues of both ^{7}Li and ^{4}He is of the order of a few micrometers. Selective uptake of boronated molecules by malignant cells is a primary concern for the success of BNCT, being the critical factor which allows to spare healthy cells while killing neoplastic ones. Various methods to obtain this goal have been developed. Strategies employed include: (i) the use of boronated compounds with some affinity for tumors, such as borophenylalanine (BPA)[3,4]; (ii) the conjugation of boron-rich molecular moieties with tumor-specific monoclonal antibodies [5,6]; and (iii) the use of carriers such as conventional, neutral liposomes to deliver boronated molecules [7–11].

The ability of delivering boron-containing compounds deeply inside the tumor cells and, possibly, close the nucleus, is also an important requirement in order to improve the efficiency of BNCT. Cationic liposomes are

* Corresponding author. Tel.: +39-55-457-3042; fax: +39-55-457-3036.
E-mail address: martini@csgi.unifi.it (G. Martini).

0005-2736/$ - see front matter © 2004 Elsevier B.V. All rights reserved.
doi:10.1016/j.bbamem.2004.04.002

currently used for delivering gene and other DNA fragments [12–16]; their ability to penetrate eucaryotic cells and to reach the nucleus has been widely demonstrated, so we thought it could be interesting to study the insertion of boro-compounds into cationic liposomes, in view of their possible use as carriers for BNCT.

The boronated molecules used in this work were the carboranyl derivatives **1**,**2**:

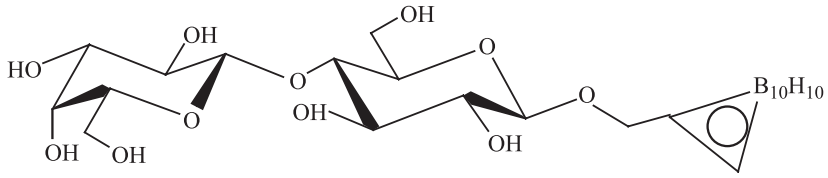

1

[1,2-dicarba-*closo*-dodecaboran(12)-1-ylmethyl](β-D-galactopyranosyl)-(1→4)-β-D-glucopyranoside] (LCOB)

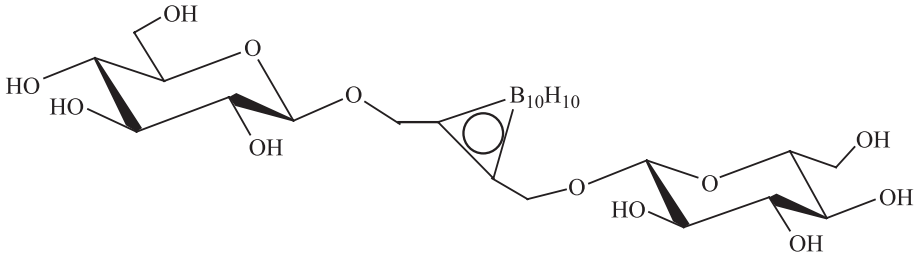

2

1,2-Di-(β-D-gluco-pyranosyl-ox)methyl-1,2-dicarba-*closo*-dodecaborane(12) (DGCOB)

These molecules consist of a cluster containing 10 boron and two carbon atoms (*closo*-carborane unit), with icoesahedral geometry, covalently attached to two sugar rings. The above molecules and similar compounds have been recently tested in vitro and in vivo as boronating agents for B-16 melanoma and C6 rat glioma cells, with encouraging results [17].

Continuous-wave Electron Spin Resonance (ESR) of appropriately tailored probes has been used to study self-assembled systems, because of its sensitivity to dynamical events in the time scale of nanoseconds or slower, and because several features, such as ordering and clustering at a molecular level, can be monitored [18–22].

Recently, the physico-chemical properties of liposomes built up with a cationic surfactant (di-oleoyltrimethylammonium propane, DOTAP, **3**) and a neutral phospholipid (L-α-dioleoylphosphatidyl-ethanolamine, DOPE, **4**) in the 1:1 weight ratio have been studied with the aid of the ESR of stable nitroxide radicals inserted into the vesicle bilayers and with the aid of Differential Scanning Calorimetry (DSC) [23].

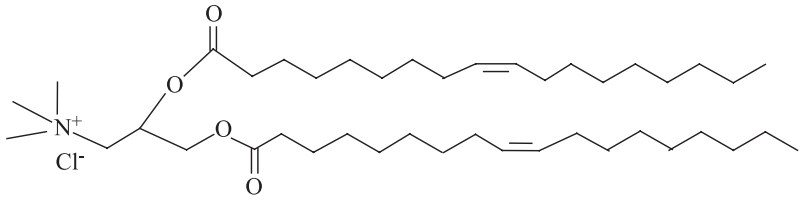

3

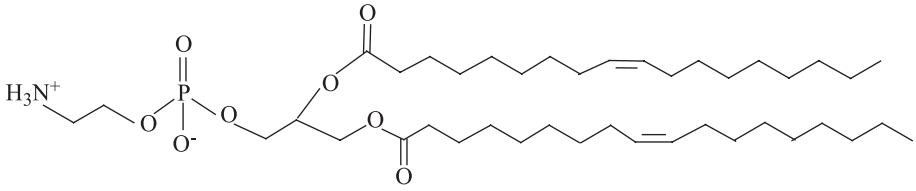

4

In this paper we report on the ESR and Light Scattering (LS) characterization of DOTAP/DOPE liposomes before and after interaction with boronated compounds.

2. Experimental section

2.1. Materials

Carboranes **1** and **2** were synthesized according to the procedure reported in Ref. [24] and used without further treatment. Both LCOB (**1**) and DGCOB (**2**) were water-soluble, at least up to 2×10^{-2} mol/l.

DOTAP (**3**) and DOPE (**4**) were purchased from Avanti-lipids, Alabama, and used as received.

The ESR probes 5-DSA (5-doxyl-stearic acid, **5**) and 16-DSA (16-doxyl-stearic acid, **6**) were obtained from Sigma Chemicals, München, Germany.

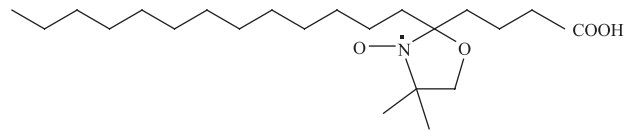

5

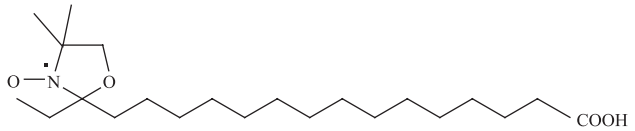

6

The working pH ensured that the DSA probes were protonated since stearic acid is a very weak acid.

2.1.1. Sample preparation

Liposomes built up with DOTAP and DOPE, in the weight ratio 1:1, were extruded with 27 passages trough polycarbonate membranes (pore diameter 100 nm) after the preparation of multilamellar dispersions, as described in Ref. [23]. PBS (phosphate buffer 10^{-2} mol/l) at pH = 7.4 and 0.15 mol/l NaCl in water were used as the aqueous medium. This procedure gave the most reproducible results. In the following, this medium will be addressed to as physiological solution, since it is considered a good model to mimic physiological ionic strength and pH.

Total lipid concentration in liposomes was 1.4×10^{-2} mol/l (~10 mg/ml). Freshly extruded liposomes had a mean diameter of 110–130 nm, as checked by Quasi Elastic Light Scattering (QELS). These values were in agreement with those reported in the literature for similar preparation procedures [25]. As explained above, the carboranes used in this work are relatively water-soluble compounds, so they were added to preformed liposomes as aqueous solutions. Equal volumes of liposomes and of carboranes, dissolved in physiological medium, were mixed and the final solutions were let to equilibrate for 15–30 min prior ESR or LS runs. The above procedure gave samples which were stable for at least 1 week. Carborane molar fractions x_{CB}, where x_{CB}=[carborane]/([carborane]+[DOPE]), ranged from 0035 to 0.66.

Samples for ESR runs contained spin probe concentration from 10^{-4} to 2×10^{-5} mol/l. The nitroxide/lipid ratio in liposomes was therefore 1:140 or lower, which reasonably ruled out both strong line broadening and strong effects on the liposome structure, as due to the presence of foreigner molecules.

2.2. Methods

ESR spectra were recorded with the aid of the Bruker ESR spectrometer model 200D operating in the X band. Spectra acquisition and handling were carried out with the ESR software from Stelar, Milan, Italy. Temperature was controlled with the Bruker VTB 3000 apparatus; accuracy was ± 0.5 K.

Spectra were computed with the NLSL program, developed by Schneider and Freed [26] and Budil et al. [27], which allowed to reproduce the ESR absorptions in different motional conditions. From the computation, the best-fit motional and order parameters were obtained. The procedure was based on the Liouville stochastic equation, where the spin Hamiltonian terms arising from electronic Zeeman and nucleus–electron coupling are included. No contributions from nuclear Zeeman effect and from nuclear quadrupole of ^{14}N were considered.

Without entering into details of the calculation procedure, which can be found elsewhere [28–30], only a few hints are given here. Since vesicles are typical examples of structures locally ordered and macroscopically disordered, the Microscopic Order Macroscopic Disorder (MOMD) model was applied in all simulations. The time-averaged order parameter S is defined by an unique axis (the director normal to the bilayer plane) along which the reorienting potential acts:

$$S = \langle D^2_{00} \rangle = \langle 1/2(3\cos^2\theta - 1) \rangle \quad (2)$$

where D^2_{00} is a Wigner rotation matrix element. In the computation, S was assumed as a fitting parameter.

The probe reorientation is anisotropic, thus parallel and perpendicular correlation times, $\tau_{\parallel}$ and $\tau_{\perp}$, were needed to correctly describe the motion of the reorienting object. The Brownian model was assumed, for which:

$$\tau_i = 1/6D_i \quad (3)$$

with D_i being the diffusion coefficient along the i direction. In bilayer-based structures, the perpendicular components

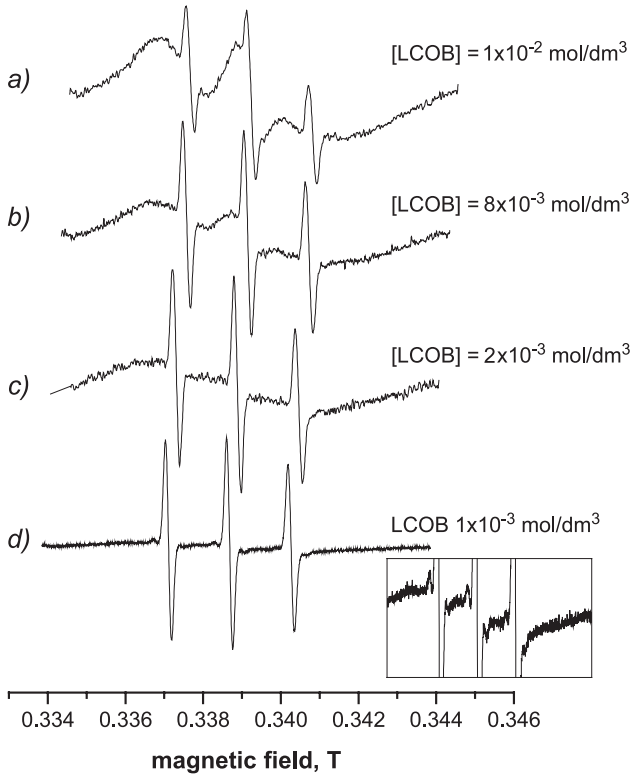

Fig. 1. ESR spectra of 5-DSA (2×10^{-5} mol/l) added to LCOB in physiological solutions at different carborane concentration ($T = 310$ K).

$\tau_{\perp}$ and $D_{\perp}$ are usually considered the more relevant ones, because they reflect the rotational wagging motion of the acyl chain long axis.

QELS experiments were performed on a Brookhaven Instrument apparatus (BI 9000AT correlator card and BI 200 SM goniometer). The signal was detected by an EMI 9863B/350 photomultiplier. The light source was the doubled frequency of a Coherent Inova diode pumped Nd-YAG laser ($\lambda = 532$ nm), linearly polarized in the vertical direction. The laser long-term power stability was $\pm 0.5\%$. Self-beating detection was recorded using decahydronaphthalene as an index matching liquid.

As it is typically done, the intensity autocorrelation function, $g_1(t)$, was fitted to a cumulant expansion of relaxation rates Γ [31] according to

$$\ln|g_1(t)| = -\overline{\Gamma}t + \frac{1}{2!}\mu_2 t^2 - \frac{1}{3!}\mu_3 t^3 + \ldots \quad (4)$$

where:

$$\overline{\Gamma} = \int_0^{\infty} \Gamma G(\Gamma) \mathrm{d}\Gamma \quad (5)$$

$G(\Gamma)$ being the weight factor that accounts for the contribution of the population with decay rate Γ to the decay of the autocorrelation function of the scattered intensity. And:

$$\mu_i = \int_0^{\infty} G(\Gamma)(\Gamma - \overline{\Gamma})^i \mathrm{d}\Gamma \quad (6)$$

A weighted least-square technique was applied to the second-order polynomial function to determine the mutual diffusion coefficient from the first cumulant, while the variance μ_2/Γ provided an evaluation of the distribution width.

Alternatively, assuming a continuous distribution of relaxation rates of the autocorrelation function, the aggregate size distribution was obtained by Laplace inversion of the experimental intensity autocorrelation function with the CONTIN algorithm [32].

3. Results and discussion

3.1. Aggregation of carboranes in solution

The carboranes studied in this work have a molecular structure reminding amphiphilic compounds, their hydrophobic and hydrophilic portions being the $B_{10}H_{10}$ cage and the sugar rings, respectively. Since drug self-association is not unusual in solution, we verified if aggregation occurs in the aqueous medium. Drug self-association is indeed dependent on temperature, ionic strength and pH, although the discontinuities in many physico-chemical properties, due to aggregate formation, are less evident and less sharp with

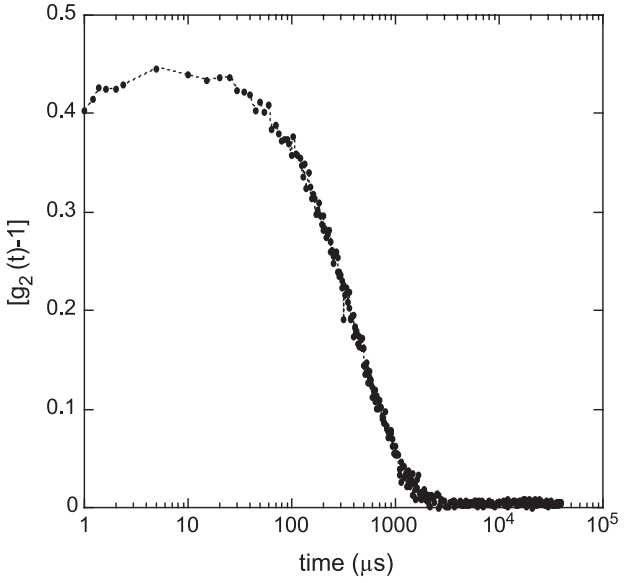

Fig. 2. Intensity autocorrelation function vs. time of a 10^{-3} mol/l LCOB in physiological solution. Scattering angle = 90°, temperature = 298 K. On the vertical axis, the normalized autocorrelation function of the scattered light $[g_2(t) - 1]$ has been reported. It is related to g_1 by the relationship: $g_2(t) = 1 + \beta|g_1(t)|^2$, where β is an instrumental parameter accounting for the signal-to-noise ratio.

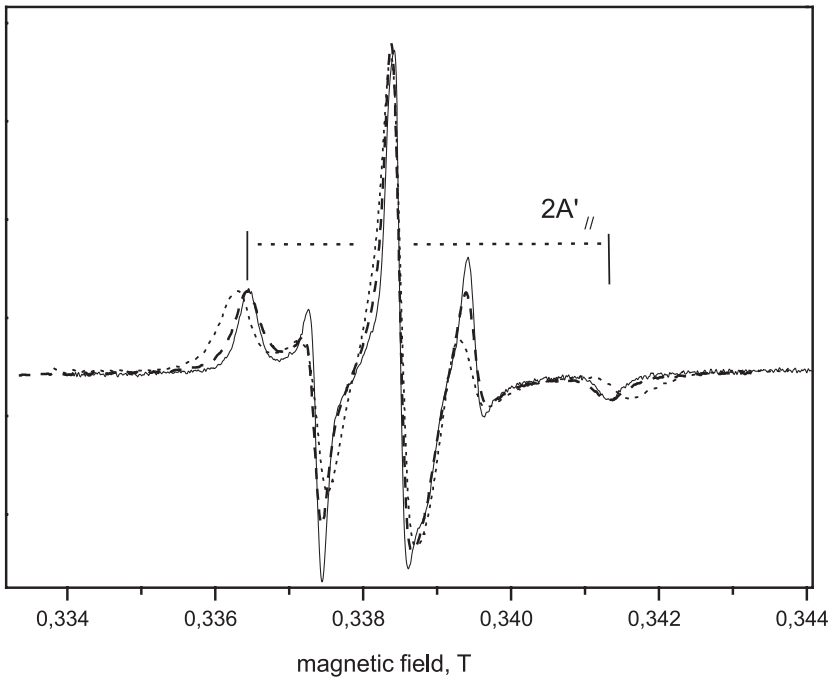

Fig. 3. 310 K ESR spectra of 5-DSA in water solution of: (*i*) carborane-free DOTAP/DOPE (w/w = 1:1) liposomes (full line); (*ii*) LCOB containing ($x_{CB} = 0.06$) DOTAP/DOPE liposomes (dashed line); (*iii*) LCOB containing ($x_{CB} = 0.67$) DOTAP/DOPE liposomes (pointed line). The calculating procedure of $2A_{||}'$ is shown in the spectrum *i*).

respect to the case of more conventional surfactants. However, the exact mechanism of drug association has long been debated, and in many instances non-cooperative pathways have been proposed [33–39].

Fig. 1 shows the experimental ESR spectra at 310 K of 5-DSA (2×10^{-5} mol/l) added to physiological solutions of LCOB at concentration between 10^{-2} mol/l (spectrum *a*) and 10^{-3} mol/l (spectrum *d*). Spectrum *d* was the well known three-line absorption of 5-DSA in almost free motion. This was simply interpreted in terms of nitroxides rapidly reorienting in an isotropic, non-viscous medium. The line shape and the hyperfine coupling constant value, $\langle A \rangle = 1.58$ mT, ensured that the environment of the probe was typically water.

A complex shape was obtained at LCOB concentration $>10^{-3}$ mol/l (spectrum *a*–*c*). In particular, spectrum *a* was dominated by a large ESR absorption due to spin probes in restricted motional conditions, superimposed to the narrow three-line absorption which is typical of nitroxides molecules in fast motional regime. The broad spectrum was therefore attributed to nitroxides inserted into carborane aggregates. The partition of spin probes between two different motional domains in slow mutual exchange is not unusual in the study of self-assembling systems, most of them having been recognized as micelles [40–47]. The three-line isotropic signal in spectrum *a* meant that a small fraction of 5-DSA probes (3–5%, as estimated from signal double integration) resided in the aqueous environment in slow exchange ($\tau_{exch} > 10^{-9}$ s) with 5-DSA embedded in carborane aggregates. As for the lowest concentration reported in the figure, aggregate presence was suggested at [LCOB] = 10^{-3} mol/l by the enlargement of spectrum *d* (inset). However, no reliable conclusions on the exact value of the aggregation concentration could be drawn for this system by ESR data only. In fact, the partition of nitroxides and the need of using low probe/carborane ratios prevented us to carry out the same analysis as in the case of more concentrated samples.

QELS was thus used to verify the presence of aggregates in dilute solution. These measurements were not performed on concentrate samples because of their translucent, slightly milky appearance. Actually, large structures were detected at concentrations as low as $6–7 \times 10^{-4}$ mol/l.

Fig. 2 shows the intensity autocorrelation function of LCOB at 10^{-3} mol/l concentration in physiological solution, obtained at a scattering angle of 90°. The above-

Table 1
Best-fit magnetic parameters used to reproduce the 310 K ESR spectra of *n*-DSA inserted in DOTAP/DOPE liposomes[a]

	g_{xx}	g_{yy}	g_{zz}	A_{xx} (mT)	A_{yy} (mT)	A_{zz} (mT)	$\tau_{\perp}$ ($s \times 10^{10}$)	*n*	S_{20}
5-DSA	2.0089	2.0060	2.0029	0.62	0.63	3.3	6.5	10	0.5
16-DSA	2.0093	2.0060	2.0024	0.59	0.6	3.25	5.0	1	0.03

[a] $n = \tau_{\perp}/\tau_{\parallel}$.

mentioned slightly opalescent aspect (which persisted to a lesser extent down to this low concentration) indicated the presence of mesoscopic scale aggregates.

A second-order cumulant fit of this autocorrelation function yielded a relaxation rate of 1.167 kHz, due to the Brownian motion of objects with a diffusion coefficient of 2.35×10^{-8} cm^2 s^{-1}, clearly inconsistent with the motion of LCOB monomers.

According to the Debye–Stokes–Einstein equation ($D = k_B T/6\pi\eta R_h$, where R_h is the particle hydrodynamic radius and η the solvent viscosity), the previous value is connected to a hydrodynamic size, which in the present case was 104 nm.

The overall behavior of DGCOB was very similar to that of LCOB.

QELS data gave therefore experimental evidence that strong aggregation in the binary systems of sugar-derived carboranes has to be taken into account when employing this kind of molecules in aqueous media.

3.2. DOTAP/DOPE liposomes loaded with carboranes

Fig. 3 shows the 310 K ESR spectra of 5-DSA in DOTAP/DOPE liposomes containing LCOB at LCOB molar fraction $x_{CB} = 0.06$ and $x_{CB} = 0.67$, as compared with the 5-DSA spectrum in the carborane-free liposomes in the same experimental conditions. As reported in ref. [23], 5-DSA inserted in the bilayer of DOTAP/DOPE liposomes in pure water gives rise to the typical spectrum of the nitroxide in restricted motion with not completely averaged magnetic anisotropies. The narrow line width observed suggests that 5-DSA probes are located in a highly uniform site distribution. No significant differences were observed in the ESR spectra when pure water was replaced by physiological solution, as it was done in this work. The same best-fit magnetic parameters were therefore used in the calculation (Table 1). A small increase of the overall spectral width, even at the lower carborane content, indicated that a less uniform environment was sensed by the probes. This was interpreted as a proof of carborane insertion. A more marked order increase and mobility decrease in the bilayer took place at high LCOB molar fraction, as it is evidenced by the data reported in Table 2, where motional and order parameters at several loading ratios are compared. Again in Fig. 3, the evaluation procedure of outer hyperfine splitting $2A_{\parallel}'$ is also shown. Fig. 4 reports the $2A_{\parallel}'$ values of 5-DSA inserted in DOTAP/DOPE liposomes, obtained at two different temperatures as a function of LCOB and DGCOB loading. $2A_{\parallel}'$ is a good semi-empirical parameter for the ESR analysis of probes located in axially anisotropic environments, since it is correlated with fluidity and molecular

Table 2
Best-fit parameters for the simulation of 5-DSA ESR spectra in DOTAP/DOPE liposomes containing different amount of LCOB

x_{CB}	n	$\tau_\perp$ ($s \times 10^{10}$)	S_{20}
0	10	6.5	0.5
0.035	10	8.6	0.51
0.067	10	9.7	0.51
0.127	5	11.1	0.51
0.176	5	13.7	0.53
0.263	5	14.0	0.53
0.391	5	15.4	0.55
0.52	5	15.9	0.58
0.66	5	18.8	0.63

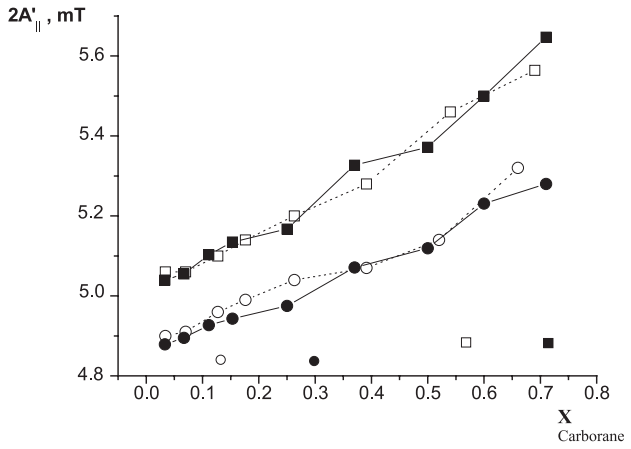

Fig. 4. Partially averaged parallel hyperfine component, $2A_{||}'$, of 5-DSA ESR spectra as a function of the carborane molar fraction in DOTAP/DOPE (w/w = 1:1) liposome dispersions: (□) LCOB, $T = 298$; (■) DGCOB, $T = 298$; (○) LCOB, $T = 310$; (●) DGCOB, $T = 310$.

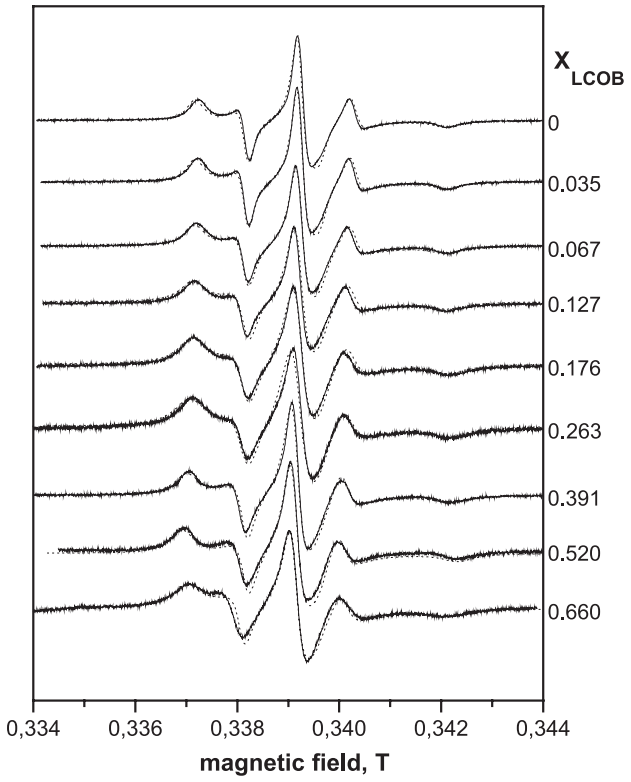

Fig. 5. Experimental (full lines) and computed (pointed lines) 310 K ESR spectra of 5-DSA in DOTAP/DOPE liposomes containing different molar fraction of LCOB.

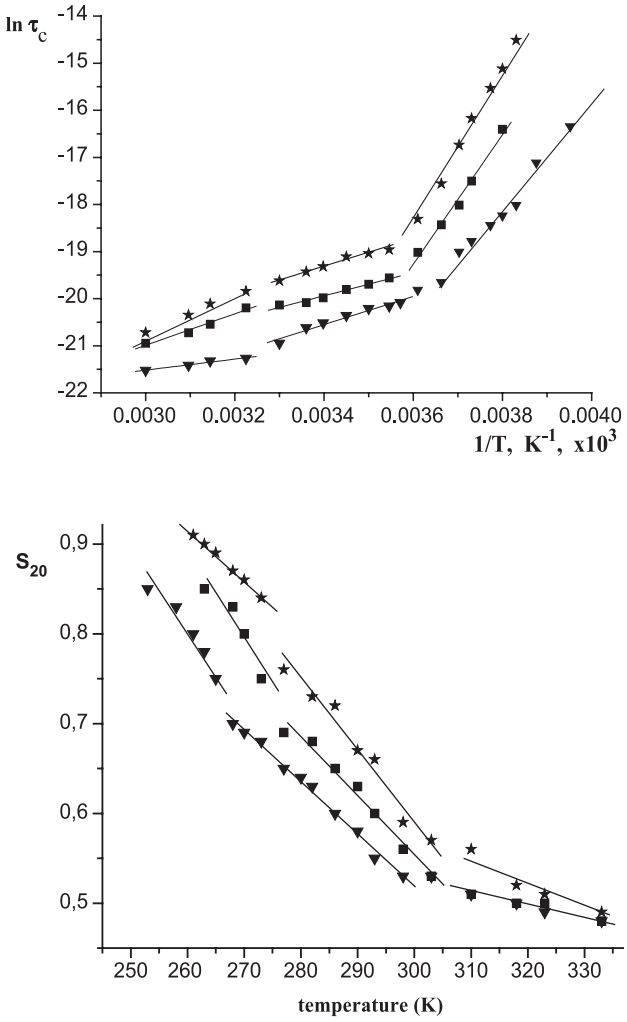

Fig. 6. Above: Temperature dependence of $\ln\tau_{\perp}$ of 5-DSA inserted in: (▼) DOTAP/DOPE liposomes in physiological solution; (■) as in ▼ with added LCOB up to $x_{CB}=0.25$; (★) as in ▼, with added LCOB up to $x_{CB}=0.5$. Bottom: Order parameter, S_{20}, of 5-DSA in: (▼) DOTAP/DOPE liposomes in physiological solution; (■) as in ▼ with added LCOB up to $x_{CB}=0.25$; (★) as in ▼, with added LCOB up to $x_{CB}=0.5$.

order. It has been extensively used to show trends and point out transitions in bilayer-based structures [48–53]. The two carboranes gave almost overlapping results, indicating that very similar interactions took place. The hydrophobic portion of the two carboranes, that is the $B_{10}C_2H_{11}$-cage, might therefore be responsible for both LCOB and DGCOB insertion, whereas the sugar moiety played a minor role in the bilayer modifications observed. Considering the good correlation between carborane content and lipid packing (as expressed by $2A_{\parallel}'$) shown in Fig. 4, extensive interactions between carboranes and liposomes could be assumed. Moreover, it is known that the $B_{10}C_2H_{11}$-cage has a high lipophilic character and no affinity for water or other polar environments [54,55].

Fig. 5 shows the experimental and computed spectra of the 5-DSA nitroxide inserted in liposome solutions which contained LCOB at molar fraction from 0.035 to 0.67. All the simulations reported in this figure were carried out assuming that the spin probe sensed a single environment and, therefore, a single absorption was used to reproduce the ESR spectra of liposomes interacting with LCOB at different molar fractions. The good agreement between experimental and simulated spectra, obtained with this hypothesis, suggested that all the carborane molecules were inserted into liposomes. This was also in line with the experimental evidence that no underlining or superimposed signal could be detected. Similar results were obtained for DGCOB.

Original micelles or other kinds of carborane aggregates were thus disrupted and the carborane molecules were associated with the liposome membrane. A quantitative evaluation of the incorporation extent is being performed through NMR spectroscopy of ^{1}H and ^{11}B, and preliminary results showed that no signal due to carborane monomer or to carborane aggregates was detected after interaction with liposomes.

Therefore, the only explanation we had to account for the observed ESR spectra was that the interaction occurring between carboranes and liposomes arose from insertion of the former molecules inside the hydrophobic core of the bilayer. Just to these features, the 5-DSA probe was sensitive. This suggestion also agreed with LS measurements, as it is discussed later in the text.

The simulation of all spectra recorded at different temperatures allowed us to separate the contributions due to motional and order parameters. Results are shown in Fig. 6a and b, where the variations of $\tau_{\perp}$ and S_{20} as a function of temperature for two different carborane content ($x_{CB}=0.25$ and $x_{CB}=0.5$) are compared with the same variations observed in plain liposomes. Marked discontinuities were evidenced in the trend of $\ln\tau_{\perp}$ in the same temperature range, that is from 269 to 272 K and 303 to 310 K, both for

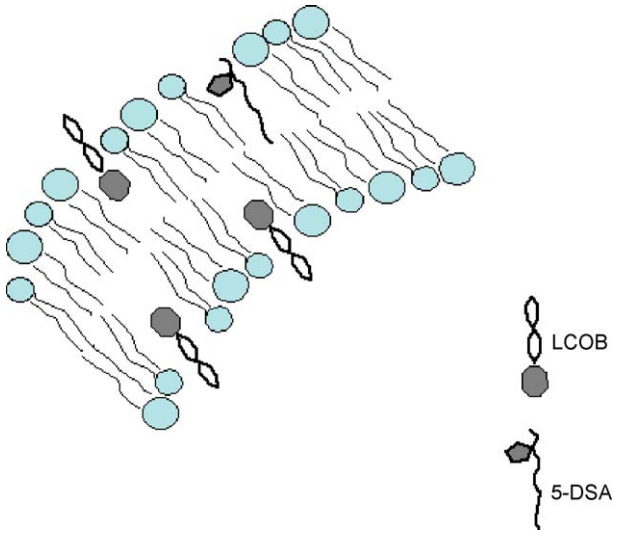

Scheme 1. Sketch of the liposome membrane bilayer after insertion of carborane (LCOB) and 5-DSA.

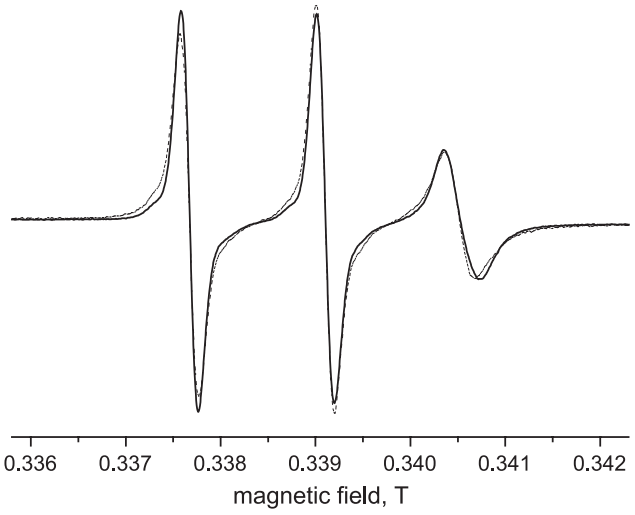

Fig. 7. ESR spectrum of 16-DSA inserted in plain DOTAP/DOPE liposomes (full line) and in liposomes containing LCOB ($x_{LCOB}=0.5$, pointed line). $T=310$ K.

drug-free and carborane loaded DOTAP/DOPE liposomes. By referring to the analysis carried out with Differential Scanning Calorimetry (DSC) data and discussed in Ref. [23], the discontinuity at lower temperature was due to the gel–liquid crystal transition of the phospholipid bilayer. DSC also suggests that only a structural rearrangement of the molecules occurs at room temperature, according to the conclusion reached by Tanaka and Freed [56]. No evidence was found for other kind of phase transition, such as lamellar-inverted hexagonal, which could in principle occur in the case of bilayers containing high amounts of DOPE

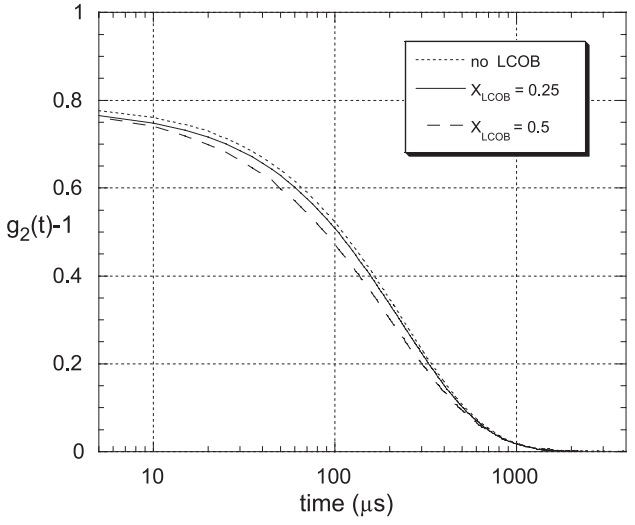

Fig. 8. Intensity autocorrelation function vs, time of DOTAP/DOPE liposomes dispersions without LCOB (pointed line) and with LCOB ($x_{LCOB}=0.25$, full line, and $x_{LCOB}=0.50$, dashed line, respectively). On the vertical axis the normalized autocorrelation function of the scattered light $[g_2(t)-1]$ has been reported. It is related to g_1 by the relationship: $g_2(t)=1+\beta|g_1(t)|^2$, where β is an instrumental parameter accounting for the signal-to-noise ratio.

Table 3a
Hydrodynamic diameter and polydispersity index for pure and LCOB-loaded liposomes

	DOTAP/DOPE liposomes	Liposomes ($+x_{CB}=0.25$)	Liposomes ($+x_{CB}=0.5$)
D_h (nm)	115	112	98
Polydispersity (%)	11	12	25

[57]. The phase transition 40–50 K above T_m is attributed by these authors to an orientational rearrangement of the hydrocarbon chains, following the Kimura and Nakano theory [58]. The same arguments could be used to explain the results reported in this work, which suggested that the contemporary presence of 5-DSA and carboranes did not deeply affect the overall behavior of the DOTAP/DOPE liposomes. In fact, from the ESR parameters analyzed in Figs. 4–6, it appeared that the basic bilayer structure of liposomes was retained, and that the fluid oleoyl chains of DOTAP and DOPE were flexible enough to host carborane cages without dramatic rearrangements. A homogeneous dissolution of both nitroxide and carborane into the liposomes could thus be assumed. A sketch of the suggested arrangements is presented in Scheme 1.

The ESR spectra of the 16-DSA spin probe showed only very small differences between unloaded liposomes and liposomes containing carboranes up to $x_{CB}=0.5–0.6$. A typical example is reported in Fig. 7 where the 310 K spectra of 16-DSA in plain liposomes and in liposomes containing LCOB at 0.5 molar fraction are compared. Taking into account that the size of lipophilic moiety for the carboranes used in this work can be estimated to be 0.7–0.8 nm [59], and that the full length of an oleoyl chain in the L_β phase is about 1.6–1.7 nm [60], the above findings demonstrated that the perturbation induced by carborane insertion was mainly limited to the region close to the polar heads of the lipid bilayer.

QELS measurements were performed on DOTAP/DOPE liposomes containing LCOB or DGCOB at different loading ratios and the results were compared with those of plain liposomes. All samples were diluted 1:20 in order to reduce optical density and to avoid multiple scattering effects. A typical trend is shown in Fig. 8, while the corresponding results are reported in Tables 3a and 3b for LCOB and DGCOB, respectively.

The intensity autocorrelation functions indicated that the decay of the refractive index fluctuations had a small, but

Table 3b
Hydrodynamic diameter and polydispersity index for pure and DGCOB-loaded liposomes

	DOTAP/DOPE liposomes[a]	Liposomes ($+x_{CB}=0.25$)	Liposomes ($+x_{CB}=0.5$)
D_h (nm)	126	125	124
Polydispersity (%)	10	10	12.5

[a] The small differences in the pure liposomes diameter and polydispersity with respect to Table 3a are due to different preparations.

appreciable and reproducible, dependence on the carborane content. This was more evident in the trend of the hydrodynamic diameter and polydispersity index, which were calculated from second-order cumulant in the fit of the decay curves.

The effects induced by LCOB insertion were slightly more marked than those obtained in the case of DGCOB insertion, but the trend of a small decrease in the liposome mean size and increase in polydispersity was common to both carboranes. The almost spherical shape of liposomes was therefore maintained after carborane insertion. Only minor effects on the bilayer curvature, which caused a smaller diameter, were observed. Finally, it should be noted that the size distribution, as measured from the second cumulant coefficient, never exceeded 25–30%. This range of values could be considered low enough to allow the description of the carborane/liposome systems as they were made by well-defined spherical objects.

Laplace inversion, performed with the program CONTIN, gave a monomodal size distribution for all samples. In no cases the simultaneous presence of two distributions with different mean size and/or different polydispersity could be evidenced.

4. Conclusion

Carboranes derivatized with two glucosyl units were shown to behave as amphiphilic compounds. They were able to form aggregates in water solution and to be inserted in the double layer of DOTAP/DOPE liposomes. Lipid packing and dynamics of liposomes, though altered by carborane insertion, did not show any dramatic change. In particular, the ESR spectra of stearic acid doxyl derivatives showed that lipid order was slightly increased in the presence of carboranes. QELS measurements evidenced that a small decrease in the liposome hydrodynamic diameter took place, together with a limited increase in polydispersity. The interaction between sugar-based carboranes and cationic liposomes did not induce any destabilization of the latter; on the contrary, the observed behavior was a less marked tendency of loaded liposomes to phase separate over time. These results are very interesting when liposomes are to be used as drug carriers because, in order to penetrate inside tumor cell, they have to retain their overall properties and, in particular, the mean diameter has to be kept in the optimal rage of 100–200 nm.

We thus conclude that DOTAP/DOPE cationic liposomes loaded with sugar-based carboranes are good candidates for boron delivery in Neutron Capture Therapy.

Acknowledgements

The authors thank the University of Florence and the Consorzio per lo Sviluppo dei Sistemi a Grande Interfase, CSGI, Italy, for financial and instrumental support.

References

[1] B. Larsson, J. Crawford, R. Weinreich (Eds.), Advances in Neutron Capture Therapy, vol. I, Elsevier, Amsterdam, 1997.
[2] R.F. Bart, A critical assessment of Boron Neutron Capture Therapy: an overview, J. Neuro-Oncol. 62 (2003) 1–5 (and reference therein).
[3] Y. Mishima, C. Honda, M. Ichihashi, H. Obara, J. Hiratsuka, H. Fukuda, H. Karashima, T. Koboyashi, K. Kanda, Treatment of malignant melanoma by single thermal Neutron Capture Therapy with melanoma-seeking ^{10}B-compound, Lancet 11 (1989) 388–389.
[4] J.A. Coderre, J.D. Glass, R.G. Fairchild, P.L. Micca, I. Fand, D.D. Joel, Selective delivery of boron by the melanin precursor analogue *p*-boronophenylalanine to tumors other than melanoma, Cancer Res. 50 (1990) 138–141.
[5] A. Varadarajan, R.M. Sharkey, D.M. Goldenberg, M.F. Hawthorne, Conjugation of phenyl isothiocyanate derivatives of carborane to antitumor antibody and in vivo localization of conjugates in nude mice, Bioconjug. Chem. 2 (1991) 102–110.
[6] C.J. Chen, R.R. Kane, F.J. Primus, G. Szlai, M.F. Hawthorne, J.E. Shively, Synthesis and characterization of oligomeric nido-carboranyl phosphate diester conjugates to antibody and antibody fragments for potential use in Boron Neutron Capture Therapy of solid tumors, Bioconjug. Chem. 5 (1994) 557–564.
[7] K. Shelly, D.A. Feakes, M.F. Hawthorne, P.G. Schmidt, T.A. Krisch, W.F. Bauer, Model studies directed toward the Boron Neutron Capture Therapy of cancer: boron delivery to murine tumors with liposomes, Proc. Natl. Acad. Sci. U. S. A. 89 (1992) 9039–9043.
[8] S.C. Mehta, J.C. Lai, D.R. Lu, Liposomal formulations containing sodium mercaptoundecahydrododecaborate (BSH) for Boron Neutron Capture Therapy, J. Microencapsul. 13 (1996) 269–279.
[9] A.M. Moraes, M.H. Santana, R.G. Carbonell, Preparation and characterization of liposomal systems entrapping the boronated compound *o*-carboranylpropylamine, J. Microencapsul. 16 (1999) 647–664.
[10] M. Johnsson, N. Bergstrand, K. Edwards, Optimization of drug loading procedures and characterization of liposomal formulations of two novel agents intended for Boron Neutron Capture Therapy (BNCT), J. Liposome Res. 9 (1999) 53–79.
[11] F. Pavanetto, P. Perugini, I. Genta, C. Minoia, A. Ronchi, U. Prati, L. Riveda, R. Nano, Boron-loaded liposomes in the treatment of hepatic metastases: preliminary investigation by autoradiography analysis, Drug Deliv. 7 (2000) 97–103.
[12] D.D. Lasic, N.S. Templeton, Liposomes in gene therapy, Adv. Drug Deliv. Rev. 20 (1996) 221–266.
[13] A.D. Miller, Cationic liposomes for gene therapy, Angew. Chem., Int. Ed. Engl. 37 (1998) 1768–1785.
[14] Y.S. Mel'nikova, S.M. Mel'nikov, J.E. Löfroth, Physico-chemical aspects of the interaction between DNA and oppositely charged mixed liposomes, Biophys. Chemist. 81 (1999) 125–141.
[15] V.M. Meidan, J.S. Cohen, N. Amariglio, D. Hirsch-Lerner, Y. Barenholz, Interaction of oligonucleotides with cationic lipids: the relationship between electrostatics, hydration and state of aggregation, Biochim. Biophys. Acta 1464 (2000) 251–261.
[16] J.A. Heynes, D. Nicolescu-Duvaz, R.G. Cooper, C.J. Springer, Synthesis of novel cationic lipids: effect of structural modification on the efficiency of gene transfer, J. Med. Chem. 45 (2002) 99–114.
[17] L.F. Tietze, U. Bothe, U. Griesbach, M. Nakaiki, T. Hasegawa, H. Nakamura, Y. Yamamoto, *Ortho*-Carboranyl glycosides for the treatment of cancer by Boron Neutron Capture Therapy, Bioorg. Med. Chem. 9 (2001) 1747–1752.
[18] D. Marsh, D. Kurad, V.A. Livshits, High-field electron spin resonance of spin labels in membranes, Chem. Phys. Lipids 116 (2002) 93–114.
[19] L.J. Korstanje, E.E. van Faassen, Y.K. Levine, Reorientational dynamics in lipid vesicles and liposomes studied with ESR: effects of

hydration, curvature and unsaturation, Biochim. Biophys. Acta 982 (1989) 196–204.
[20] Z.-C. Liang, P.-O. Westlund, G. Wikander, G. Lindbloem, A quantitative Electron Spin Resonance line shape study of order–disorder transition in the lamellar phase of the palmitoyllysophosphatidylcholine–water system, Mol. Phys. 85 (1995) 757–767.
[21] J. Štrancar, M. Šentjurc, M. Schara, Fast and accurate characterization of biological membranes by EPR spectral simulations of nitroxides, J. Magn. Reson. 142 (2000) 254–265.
[22] C.R. Benatti, E. Feitosa, R.M. Fernandez, M.T. Lamy-Freund, Structural and thermal characterization of dioctadecyldimethylammonium bromide dispersions by spin labels, Chem. Phys. Lipids 11 (2001) 93–104.
[23] I. Perissi, S. Ristori, S. Rossi, L. Dei, G. Martini, Electron spin resonance and differential scanning calorimetry as combined tools for the study of liposomes in the presence of long chain nitroxides, J. Phys. Chem., B 106 (2002) 10468–10473.
[24] G.B. Giovenzana, L. Lay, D. Monti, G. Palmisano, L. Panza, Synthesis of carboranyl derivatives of alkynyl glycosides as potential BNCT agents, Tetrahedron 55 (1999) 14123–14136.
[25] R.C. MacDonald, R.I. MacDonald, B.Ph.M. Menco, K. Takeshta, N.K. Subbarao, L. Hu, Small-volume extrusion apparatus for preparation of large, unilamellar vesicles, Biochim. Biophys. Acta 1061 (1991) 297–303.
[26] D.J. Schneider, J.H. Freed, Calculating slow motional magnetic resonance spectra: a user's guide, in: L.J. Berliner, J. Reuben (Eds.), Biological Magnetic Resonance. Spin Labeling. Theory and Applications, vol. 8, Plenum, New York, 1989, pp. 1–76.
[27] D.E. Budil, S. Lee, S. Saxena, J.H. Freed, Nonlinear-least-square analysis of slow-motion EPR spectra in one and two dimensions using a modified Levenberg–Marquardt algorithm, J. Magn. Reson., Ser. A 120 (1996) 155–189.
[28] E. Meirovitch, A. Nayeem, J.H. Freed, Analysis of protein–lipid interactions based on model simulations of electron spin resonance spectra, J. Phys. Chem. 88 (1984) 3454–3465.
[29] M. Ge, J.H. Freed, Electron spin resonance study of aggregation of gramicidin in dipalmitoylphosphatidylcholine bilayers and hydrophobic mismatch, Biophys. J. 76 (1999) 264–280.
[30] Z. Jingyan, Z. Luz, H. Zimmerman, D. Goldfarb, The formation of the mesoporous material MCM-41 as studied by EPR line shape analysis of spin probes, J. Phys. Chem. 104 (2000) 279–285.
[31] D.E. Koppel, Analysis of macromolecular polydispersity in intensity correlation spectroscopy: the methods of cumulants, J. Chem. Phys. 57 (1972) 4814–4820.
[32] S.W. Provencher, A constrained regularization method for inverting data represented by linear algebraic or integral equations, Comput. Phys. Commun. 27 (1982) 213–227.
[33] D. Attwood, The mode of association of amphiphilic drugs in aqueous solution, Adv. Colloid Interface Sci. 55 (1995) 271–303.
[34] F. Gaboriau, M. Chéron, L. Leroy, J. Bolard, Physico-chemical properties of the heat-induced super-aggregates of amphotericin B, Biophys. Chem. 66 (1997) 1–12.
[35] A.D. Atherton, B.W. Barry, Photon correlation spectroscopy of surface active cationic drugs, J. Pharm. Pharmacol. 37 (1985) 854–862.
[36] D. Attwood, R.J. Natarajan, Effect of pH on the micellar properties of amphiphilic drugs in aqueous solution, J. Pharm. Pharmacol. 33 (1981) 136–140.
[37] M. Gagos, R. Koper, W.I. Gruszecki, Spectrophotometric analysis of organisation of dipalmitoylphosphatidylcholine bilayers containing the polyene antibiotic amphotericin B, Biochim. Biophys. Acta 1511 (2001) 90–98.
[38] C.E. Soma, C. Dubernet, D. Bentolila, S. Benita, P. Couvreur, Reversion of multidrug resistance by co-encapsulation of doxorubicin and cyclosporin A in polyalkylcyanoacrylate nanoparticles, Biomaterials 21 (2000) 1–7.
[39] P. Taboada, J.M. Ruso, M. Garcia, V. Mosquera, Surface properties of some amphiphilic antidepressant drugs, Colloids Surf., A Physicochem. Eng. Asp. 179 (2001) 125–128.
[40] S. Schreier, S.V.P. Malheiros, E. De Paula, Surface active drugs: self-association and interaction with membranes and surfactants. physicochemical and biological aspects, Biochim. Biophys. Acta 1508 (2000) 210–234.
[41] G. Wikander, L.B.A. Johansson, Micelle size determined by electron spin resonance and fluorescence spectroscopy, Langmuir 5 (1989) 728–733.
[42] S. Ristori, G. Martini, Electron paramagnetic resonance line shape analysis of small and large probes introduced into micellar aqueous solutions of ammonium pentadecafluorooctanoate, Langmuir 8 (1992) 1937–1942.
[43] S. Kutsumizu, S. Schlick, Self-assembling of ethylene-methacrylic acid ionomers in aqueous solutions and as swollen membranes, from ESR spectra of amphiphilic spin probes: 1. Structure of aggregates and effect of ionomer concentration, Macromolecules 30 (1997) 2320–2328.
[44] M.F. Ottaviani, P. Baglioni, G. Martini, Micellar solutions of sulfate surfactants studied by electron spin resonance of nitroxide radicals. Part 1. Use of neutral and positively charged spin probes, J. Phys. Chem. 87 (1983) 3146.
[45] Y. Wang, D. Lu, C. Long, B. Han, H. Yan, Interactions between sodium dodecyl sulfate and hydrophobically modified poly(acrylamide)s studied by electron spin resonance and transmission electron microscopy, Langmuir 14 (1998) 2050–2054.
[46] H. Caldararu, Structural aspects in self-assembled systems of polyoxyethylene surfactants, as studied by the spin probe technique, Spectrochim. Acta, Part A: Mol. Biomol. Spectrosc. 54 (1998) 2309–2336.
[47] I. Dragutan, V. Dragutan, A. Caragheorgheopol, A.K. Zarkadis, H. Fisher, H. Hoffmann, Nitroxide spin probes for magnetic resonance characterization of ordered systems, Colloids Surf., A Physicochem. Eng. Asp. 183–5 (2001) 767–776.
[48] R. Bartucci, M. Pantusa, D. Marsh, L. Sportelli, Interaction of human serum albumin with membranes containing polymer-grafted lipids: spin-label ESR studies in the mushroom and brush regimes, Biochim. Biophys. Acta 1564 (2002) 237–242.
[49] M.P. Veiga, J.L.R. Arrondo, F.M. Goòi, A. Alonso, D. Marsh, Interaction of cholesterol with sphingomyelin in mixed membranes containing phosphatidylcholine, studied by spin-label ESR and IR spectroscopies. A possible stabilization of gel-phase sphingolipid domains by cholesterol, Biochemistry 40 (2001) 2614–2622.
[50] G. Montesano, R. Bartucci, S. Belsito, D. Marsh, L. Sportelli, Lipid membrane expansion and micelle formation by polymer-grafted lipids: scaling with polymer length studied by spin-label electron spin resonance, Biophys. J. 80 (2001) 1372–1383.
[51] M.P. Veiga, F.M. Goòi, A. Alonso, D. Marsh, Mixed membranes of sphingolipids and glycerolipids as studied by spin-label ESR spectroscopy. A search for domain formation, Biochemistry 39 (2000) 9876–9883.
[52] K. Tajima, Y. Imai, T. Horiuchi, M. Koshinuma, A. Nakamura, ESR Study on DMPC and DMPG Bilayers in the (Lα + H2O) phase, Langmuir 12 (1996) 6651–6658.
[53] S. Szabó, M. Budai, K. Blaskó, P. Gróf, Molecular dynamics of cyclic lipodepsipeptides' action on model membranes: effects of syringopeptin 22A, syringomicin E, and syringotoxin studied by EPR technique, Biochim. Biophys. Acta 1660 (2004) 118–120.
[54] J.L. Fauchère, K.Q. Do, P.Y.C. Jow, C. Hansch, Unusually strong lipophilicity of 'fat' or 'super' amino-acids, including a new reference value for glycine, Experientia 36 (1980) 1203–1204.
[55] K. Yamamoto, Y. Endo, Utility of boron clusters for drug design. Hansch–Fujita hydrophobic parameters π of dicarba-*closo*-dodecaboranyl groups, Bioorg. Med. Chem. Lett. 11 (2001) 2389–2392.
[56] H. Tanaka, J.H. Freed, Electron Spin Resonance studies on ordering and rotational diffusion in oriented phosphatidylcholine multilayers:

evidence for a new chain-ordering transition, J. Phys. Chem. 88 (1984) 6633–6644.
[57] C.R. Safinya, Structures of lipid–DNA complexes: supramolecular assembly and gene delivery, Curr. Opin. Struck. Biol. 11 (2001) 440–448.
[58] H. Kimura, H. Nakano, Successive phase transitions in lipid membranes, Mol. Cryst. Liq. Cryst. 68 (1981) 289–299.
[59] J.F. Valliant, K.J. Guenther, A.S. King, P. Morel, P. Shaffer, O.O. Sogbein, K.A. Stephenson, The medicinal chemistry of carboranes, Coord. Chem. Rev. 232 (2002) 173–230.
[60] G. Cevc, Phospholipids Handbook, Marcel Dekker, New York, 1993.